Pulse Experiments as a Prerequisite for the Quantification of in Vivo Enzyme Kinetics in Aromatic Amino Acid Pathway of *Escherichia coli*

M. Schmitz,[†] E. Hirsch,[†] J. Bongaerts,[‡] and R. Takors*[,†]

Institute of Biotechnology 2, Research Centre Jülich, 52425 Jülich, Germany, and DSM Biotech GmbH, Karl-Heinz-Beckurts-Str. 13, 52428 Jülich, Germany

Glucose pulse experiments were performed to elucidate their effects on the carbon flux into the aromatic amino acid pathway in different *Escherichia coli* strains. Using a 3-deoxy-D-*arabino*-heptulosonate 7-phosphate (DAHP, *aroB*$^-$)-producing strain, a fed-batch fermentation strategy specialized for glucose pulse experiments was developed and further applied for 3-dehydroshikimate (DHS, *aroE*$^-$)- and shikimate 3-phosphate (S3P, *aroA*$^-$)-producing *E. coli* strains. The strains overexpress a feedback-resistant DAHP synthase and additional enzymes to prevent rate-limiting steps in the aromatic amino acid pathway. Changes of carbon flux into the aromatic amino acid pathway were determined via extracellular metabolite accumulations using ^{1}H NMR and HPLC measurements. As an important result, a close relationship between pulse intensity and aromatic metabolite formation rates was identified. The more downstream an aromatic pathway intermediate was located, the stronger the glucose pulse intensity had to be in order to detect significant changes in product formation. However, with the experimental conditions chosen, changes after pulse were detected even for shikimate 3-phosphate, the most downstream accumulating metabolite of this experimental series. Hence glucose pulse experiments are assumed to be a promising tool even for the analysis of final pathway products such as, for example, L-phenylalanine.

Introduction

Pulse experiments, for instance using glucose as the sole carbon source, have been carried out in the past to identify the metabolism dynamics of *Saccharomyces cerevisiae* (*1*, *2*), *Escherichia coli* (*3*), or *Zymomonas mobilis* (*4*). Cells were cultivated in a glucose-limited steady state before a quick glucose pulse changed extracellular concentration significantly. Rapid sampling together with an inactivation of bacterial metabolism enabled further sample analysis for the identification of changing metabolite concentrations. Metabolite courses shortly after stimulation represented the basis for detailed modeling aiming at the identification of in vivo enzyme kinetic parameters of a metabolism model (*2*) that consisted of a set of ordinary differential equations.

Once a model had been identified, it could be used to simulate metabolism reaction rates that correspond to intracellular carbon fluxes. Furthermore, metabolic regulation effects could be studied that were quantified with the aid of flux control coefficients (FCC) based on the model predictions (*5*−*7*).

To date, pulse experiments have been performed with special focus on central metabolism including glycolysis, pentose-phosphate pathway, and citric cycle. However, to fully exploit the potential of this approach, it should not be limited to the analysis of central metabolism alone but should also be used to elucidate regulations of branching biosynthetic pathways such as those for amino acid synthesis. Hence, it should be ensured that pulse stimulations of central metabolism are detectable in the biosynthetic pathways of interest. Experiments should therefore be performed to investigate whether and how, for instance, glucose pulses are transmitted via central metabolism to the intermediates of the pathway of interest.

In this study, the aromatic amino acid pathway (Figure 1) was chosen as a target because the amino acids of this pathway, L-tyrosine (L-tyr), L-tryptophan (L-trp), and L-phenylalanine (L-phe), are of particular interest as precursors for chemical and pharmaceutical products. While L-trp and L-tyr were produced on a scale of 500 and 140 tons in 1998 (*8*), L-phe production was 11000 tons in 1998 and its sales are expected to be US$ 850 million for 2004 (*9*).

Aromatic amino acid synthesis starts with the precursors erythrose 4-phosphate (E4P) and phosphoenolpyruvate (PEP), which are delivered by the pentose-pathway and glycolysis, respectively (*10*). As PEP is used as a phosphate donor for glucose uptake via the phosphoenol pyruvate:carbohydrate phosphotransferase system (*11*) a shift of glucose uptake due to changing extracellular glucose levels after pulse was expected to directly affect the carbon flux into the aromatic amino acid pathway.

Glucose pulse experiments focusing on the aromatic amino acid pathway of *E. coli* would usually include the in vivo measurements of pathway intermediates directly after pulse. Although enzymatic (*1*, *3*) as well as LC-MS/

* To whom correspondence should be addressed. Ph: +49-2461-61 3365. Fax: +49-2461-61 3870. E-mail: r.takors@fz-juelich.de.
[†] Institute of Biotechnology 2.
[‡] DSM Biotech GmbH.

10.1021/bp010199z CCC: $22.00
Published on Web 08/21/2002

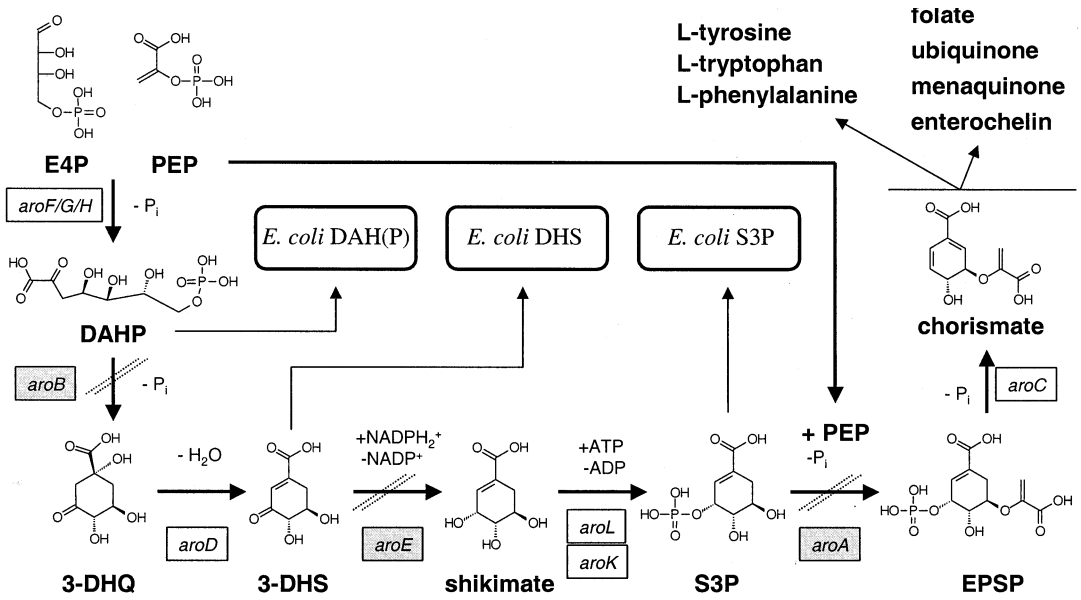

Figure 1. Strains used and their classification in the aromatic biosynthesis pathway. *E. coli* DAH(P) is an *aroB*$^-$ strain producing DAH(P), *E. coli* DHS is an *aroE*$^-$ strain producing DHS, and *E. coli* S3P is an *aroA*$^-$ strain. L-Phe is synthesized via phenylpyruvate starting from chorismate.

Table 1. *E. coli* Strains and Plasmids Used

strains, plasmids	relevant characteristics	origin and references
	E. coli Strains	
F5	LJ110 *aroB351*	Krämer, 2000 (*15*)
AB2834	λ^- *glnV42*(AS) *tsx-352 malT352*(λ^R) *aroE353*	Pittard, 1966 (*13*)
AB2829	λ^- *glnV42*(AS) *aroA354*	Pittard, 1966 (*13*)
	Plasmids	
pJF119EH	amp^R, cloning vector	Fürste, 1986 (*16*)
pF15	pJF119EH-*aroF*^{fbr}	Jossek, 2001 (*17*)
pF42	pJF119EH-*aroF*^{fbr}-*aroB*	this work
pF84	pJF119EH-*aroF*^{fbr}-*aroB-aroL*	this work

MS-based (*12*) analytical approaches have been developed for metabolites of central metabolism, these technologies could not easily be transferred because of the lack of commercially available enzymes and standards. Alternatively, three different *E. coli*-based strains producing 3-deoxy-D-*arabino*-heptulosonate 7-phosphate (DAHP), 3-dehydroshikimate (DHS), or shikimate 3-phosphate (S3P) were used to study whether their production rates were significantly affected by glucose pulses.

Materials and Methods

Culture Medium. All solutions were prepared in deionized water. Seed medium (1 L) contained $MgSO_4 \cdot 7H_2O$ (0.3 g), $CaCl_2 \cdot 2H_2O$ (0.015 g), KH_2PO_4 (3 g), K_2HPO_4 (12 g), NaCl (0.1 g), $(NH_4)_2SO_4$ (5 g), $FeSO_4 \cdot 7H_2O$ (0.075 g), Na_3-citrate$\cdot 2H_2O$ (1 g), glucose (5 g), trace element solution (1.5 mL), vitamin B1·HCl (0.0075 g), L-tyr (0.08 g), L-phe (0.7 g), L-trp (0.35 g), 4-aminobenzoic acid (0.01 g), 2,3-dihydroxybenzoic acid (0.01 g), 4-hydroxybenzoic acid (0.01 g), and ampicillin (0.1 g). The pH was adjusted to 6.5 using 25% NH_4OH. Fermentation medium (1 L) contained $MgSO_4 \cdot 7H_2O$ (3 g), $CaCl_2 \cdot 2H_2O$ (0.015 g), KH_2PO_4 (3 g), NaCl (1 g), $(NH_4)_2SO_4$ (5 g), $FeSO_4 \cdot 7H_2O$ (0.1125 g), Na_3-citrate$\cdot 2H_2O$ (1.5 g), glucose (15 g), trace element solution (1.5 mL), vitamin B1·HCl (0.0075 g), L-tyr (0.7 g), L-phe (0.7 g), L-trp (0.35 g), 4-aminobenzoic acid (0.01 g), 2,3-dihydroxybenzoic acid (0.01 g), 4-hydroxybenzoic acid (0.01 g), and ampicillin (0.1 g). The pH was adjusted to 6.5 using 25% NH_4OH. Trace element solution (1 L) contained $Al_2(SO_4)_3 \cdot 18H_2O$ (2 g), $CoSO_4 \cdot 7H_2O$ (0.75 g), $CuSO_4 \cdot 5H_2O$ (2.5 g), H_3BO_3 (0.5 g), $MnSO_4 \cdot H_2O$ (24 g), $Na_2MoO_4 \cdot 2H_2O$ (3 g), $NiSO_4 \cdot 6H_2O$ (2.5 g), $ZnSO_4 \cdot 7H_2O$ (15 g). Glucose feed solution contained 500 g/L glucose·H_2O. As indicated, isopropyl β-D-thiogalactoside (IPTG) was added to a final concentration of 100 μM, and antifoaming agent S289 (Sigma) was added as needed. All components were sterilized using standard procedures.

Bacterial Strains and Plasmids. The *E. coli* strains and plasmids used in this study are shown in Table 1. *E. coli* AB2834 (*13*) and *E. coli* AB2829 (*13*) mutants lacking catalytically active shikimate dehydrogenase (AroE) and 5-enolpyruvoylshikimate 3-phosphate synthase (AroA), respectively, were obtained from the *E. coli* Genetic Stock Center at Yale University. *E. coli* F5 is a derivative of *E. coli* K12 LJ110 (*14*), which contains a catalytically inactive 3-dehydroquinate synthase (AroB) (*15*). Hence, these strains are auxotrophic for aromatic substances and the supply with L-phe, L-tyr, and L-trp is used for control of growth during the fermentation experiment. Fermentation medium contains 4-aminobenzoic acid, 2,3-dihydroxybenzoic acid, and 4-hydroxybenzoic acid to ensure that growth is not limited by other aromatic compounds except the aromatic amino acids.

Plasmids pF15, pF42, and pF84 were based on pJF119EH (*16*), an expression vector that contains an ampicillin resistance gene and an IPTG inducible *tac*-promotor. All plasmids included the gene *aroF*^{fbr} (*17*), encoding the L-tyr feedback-resistant DAHP synthase, which was overexpressed to enhance flux into the aromatic amino acid pathway. Because of their known rate-limiting character (*18*) additionally *aroB* and *aroB* in

conjunction with *aroL* (coding for shikimate kinase II) were expressed in strains AB2834/pF42 (*E. coli* DHS) and AB2829/pF84 (*E. coli* S3P), respectively, to prevent an unwanted accumulation of upstream intermediates. These strains differ in respect to the position of the inactive enzyme in the aromatic amino acid pathway. In strain F5/pF15 (*E. coli* DAH(P)) only the first step leading to DAHP is possible, *E. coli* DHS is capable of performing the first three steps to DHS, and in *E. coli* S3P the first five steps to S3P are possible (Figure 1).

Analysis of Fermentation Medium. Samples (4 mL) of cell suspension were taken at timed intervals (4−6 samples per h in phases II and III). Glucose concentration (ACCUTREND Sensor, Roche Diagnostics) and pH were measured immediately after sampling. Cell densities were determined by measuring the absorbance at 650 nm (OD_{650}) and dry cell weight (DCW) using a 0.22-μm filter. A correlation of DCW = OD_{650} × 0.43 g/L was found. A 2-mL sample of cell suspension was centrifuged at 13,000*g* for 10 min, and the supernatant was stored at −25 °C prior to use. For ^{1}H NMR 400 μL of culture supernatant was concentrated to dryness in a vacuum centrifuge and was redissolved in deuterium oxide (D_2O) containing 4 mM of the sodium salt of 3-(trimethylsilyl)-propionic-2,2,3,3-d_4 acid, TSP (Lancaster). Concentration of DAHP and its dephosphorylated derivative DAH in the NMR sample was calculated by a comparison of integrals of metabolites with the integral of the TSP standard signal (δ = 0 ppm). All ^{1}H NMR spectra were recorded on a Bruker AMX300 FT-NMR spectrometer (300 MHz). DHS and shikimate (Sigma) were measured using HPLC with an Aminex HPX-87H column (Biorad) at 40 °C with 0.5 mL/min 0.1 N H_2SO_4 and detection at 215 nm (*19*). DHS was purified from the culture supernatant of *E. coli* DHS as described previously (*18*). S3P was measured indirectly by converting it into shikimate with the aid of the enzyme alkaline phosphatase (Roche Diagnostics) and then corrected for the in vivo produced shikimate.

Fermentation. Cryocultures were stored in Luria-Bertani (LB) medium containing 50% glycerol at −80 °C. The seed medium (150 mL) was inoculated with 2 mL of cryoculture and cultivated in a shake flask incubator at 37 °C and 160 rpm up to an OD_{650} of 3−4 and was then transferred to the bioreactor. Fed-batch fermentation was performed in a 2-L Labfors bioreactor (Infors, Switzerland) at a temperature of 37 °C; concentrated NH_4OH was used to maintain pH 6.5. Oxygen and carbon dioxide in the exhaust gas was measured using a BINOS 100 2M System (Rosemount, Germany). Dissolved oxygen (DO) was determined with an amperometric electrode (Mettler-Toledo, Germany). Data acquisition was performed via a Windows computer system running MEDUSA, an in-house software development. Glucose pulse was added manually via a syringe using a 0.22-μm filter. Glucose feed was realized with a Dosimat 665 (Metrohm AG, Switzerland).

Results and Discussion

Establishment of Experimental Method. To identify the effects of glucose pulses on the *E. coli* strains used, an experimental procedure had to be developed allowing different glucose limitation levels to be controlled and their impact on strain physiology after glucose pulses to be qualified. Using the DAH(P)-producing *E. coli* strain as an example, the fermentation strategy is described as follows. The fermentation process consisted of three phases (Figure 2). During the first phase (I) biomass was produced until the aromatic amino acids L-phe, L-tyr, and L-trp were depleted. IPTG was added

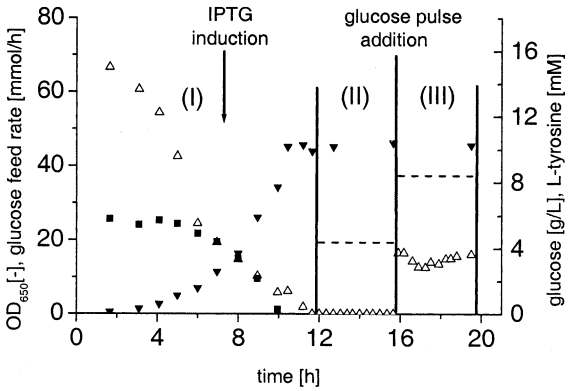

Figure 2. Fermentation process and its division into three phases for a 50% limitation experiment with *E. coli* DAH(P): (△) glucose, (■) L-tyrosine, (▼) OD_{650}, (- - -) glucose feed rate in phase II + III.

to overexpress plasmid-encoded genes to enhance carbon flux into aromatic amino acid pathway. In the second phase (II), the glucose feed was reduced to a limiting value, followed by an increase in the third phase (III) to ensure a saturated glucose supply. In phases II and III no biomass was produced. During phase I the DO was maintained above 30% and during phase II and phase III a DO setpoint of 60% and 40% of air saturation, respectively, was chosen.

To investigate the effects of glucose pulse on different glucose limitation levels, the strain-specific glucose consumption rate in phase III was estimated in a previous experiment. For *E. coli* DAHP the glucose consumption rate was determined as 37.9 mmol/h and for *E. coli* DHS and *E. coli* S3P as 78.8 and 30.3 mmol/h, respectively. All three strains achieved biomass concentrations of 19.7 g/L. For instance, taking the observed glucose consumption rate of *E. coli* DAH(P) (37.9 mmol/h) as a reference, 0%, 25%, 50%, and 75% glucose limiting feeds were calculated leading to the corresponding glucose feed rates of 37.9, 28.4, 19.0, and 9.5 mmol/h, which were used in the experiments during phase II. After about 4 h, 25 mL of a glucose solution was rapidly added to end the limitation phase (II) and to immediately shift concentration up to 5 g/L (27.6 mM). At the same time, glucose feed was increased to the determined 0% limitation value. During this third phase a DO of 40% was maintained. To investigate the effects of changing glucose supply the extracellular accumulation of pathway intermediates was measured.

Experiments with *E. coli* DAH(P). With strain *E. coli* DAH(P), pulse experiments with 25%, 50%, and 75% limitation as described above were performed. Each experiment was replicated. Figure 3 shows the production of DAH(P) before, during, and after glucose limitation. The data indicate a dependency of the rate of DAH(P) synthesis on the degree of glucose limitation (Table 2): the weaker the glucose limitation in phase II, the greater the rate of DAH(P) production. In accordance with the saturated glucose supply in phase III, the highest production rate was observed in this phase.

From the varying levels of DAH(P) formation rates we conclude that glucose pulse experiments were able to significantly change fluxes in the aromatic amino acid pathway and that the rate of formation of DAH(P) depends on the supply of glucose. The stronger the glucose limitation before the glucose pulse was set, the larger the observed flux changes were. Phase III after the glucose pulse was characterized in all experiments by a highly reproducible biomass-specific DAH(P) pro-

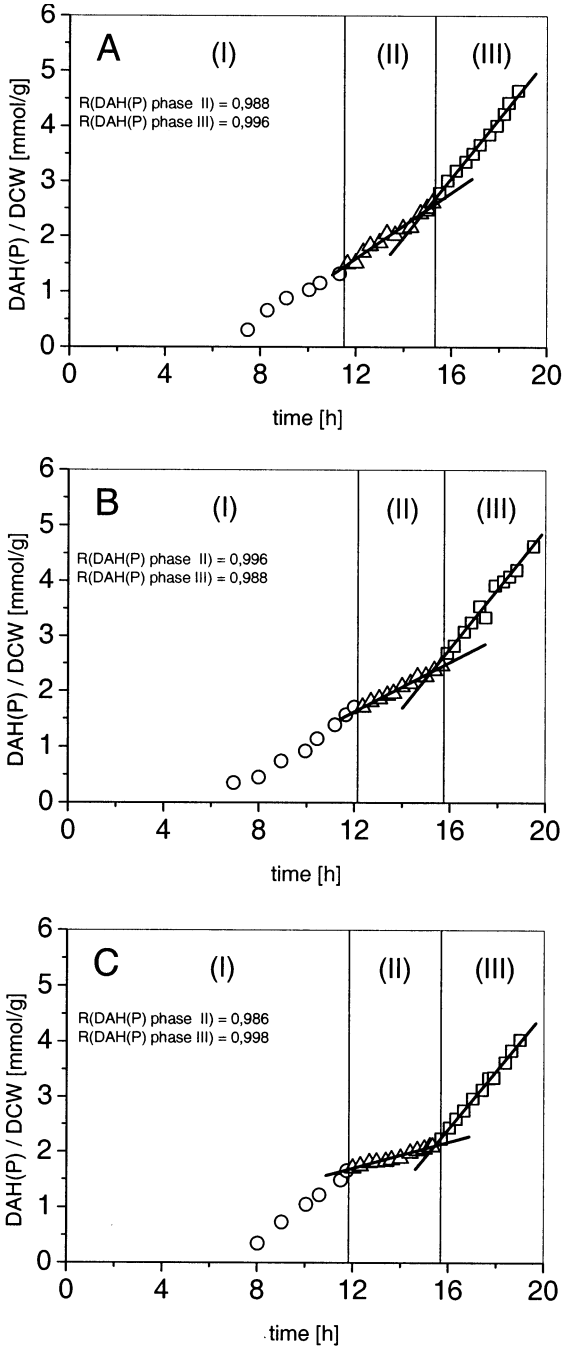

Figure 3. Biomass-specific product concentrations of *E. coli* DAH(P) in fed-batch process with glucose pulse experiments using (A) 25% glucose limitation, (B) 50% glucose limitation, and (C) 75% glucose limitation. The first (○), second (△), and third (□) phases are indicated. Line graphs represent the linear fitted data; (R) coefficient of correlation.

ductivity (Table 2), irrespective of the extent of the previous limitation. Obviously, cell metabolism was not irreversibly affected by strong glucose limitation in phase II. In all six experiments the same final DAH(P) formation rate of 0.531 ± 0.014 mmol DAH(P)/(g·h) was achieved. With respect to the parameters investigated, the strength of glucose limitation during the second phase seems to have no negative impact on the cells metabolism. From this we conclude that a highly reproducible fermentation experiment was established to investigate the influence of glucose pulses on the flux in the aromatic amino acid pathway.

Experiments with *E. coli* DHS. To study the effects of glucose dynamics using *E. coli* DHS, pulse experiments

Table 2. Specific DAH(P) Production Rates for *E. coli* DAH(P)

	limitation			
	75%	50%	25%	0%
$\pi_{DAH(P)}$[a]	0.118	0.224	0.299	0.531[c]
	0.122	0.221	0.348	
$\bar{\pi}_{DAH(P)}$[b]	0.120	0.223	0.324	0.531[c]
sd[d]	0.003	0.002	0.035	0.014[c]

[a] Specific DAH(P) production rate in mmol DAH(P)/(g·h). [b] Mean value of $\pi_{DAH(P)}$. [c] For phase III from all six experiments. [d] Standard deviation.

Table 3. Specific DHS Production Rates for *E. coli* DHS

	limitation			
	75%	50%	25%	0%
π_{DHS}[a]	0.183	0.488	n.d.[b]	0.647[c]
	0.107	0.516		
$\bar{\pi}_{DHS}$[d]	0.145	0.502	n.d.[b]	0.647[c]
sd[e]	0.054	0.020		0.017

[a] Specific DHS production rate in $mmol_{DHS}$/(g·h). [b] Not determined. [c] For phase III from all four experiments. [d] Mean value of π_{DHS}. [e] Standard deviation.

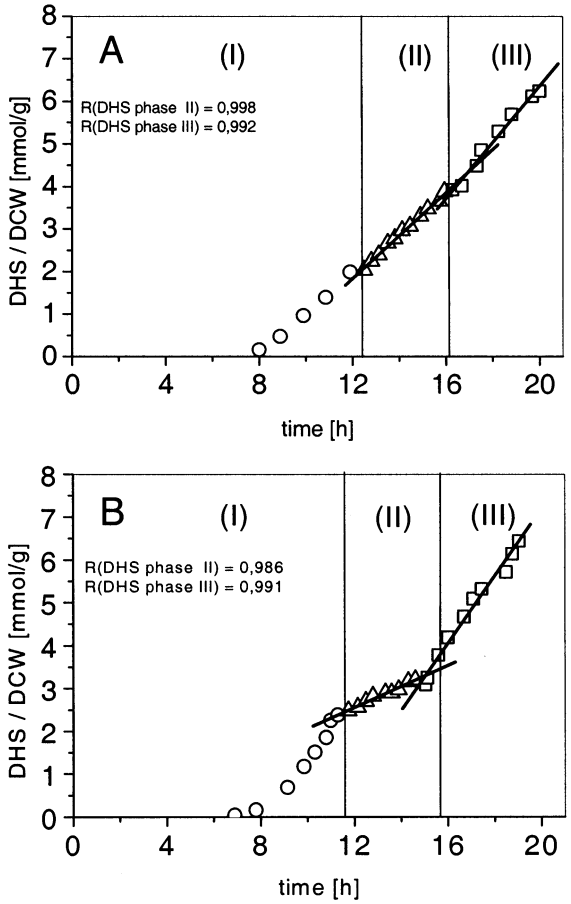

Figure 4. Biomass-specific product concentrations of *E. coli* DHS in fed-batch process with glucose pulse experiments using (A) 50% glucose limitation, (B) 75% limitation. The first (○), second (△), and third (□) phases are indicated. Line graphs represent the linear fitted data; (R) coefficient of correlation.

with 50% and 75% limitation were conducted. Each experiment was replicated. With respect to the correlation of glucose pulse intensity and DHS formation, results similar to those of the *E. coli* DAH(P) experiments were found (Table 3, Figure 4): the stronger the glucose limitation, the larger the difference in productivity after glucose pulse in the saturated third phase. However, if

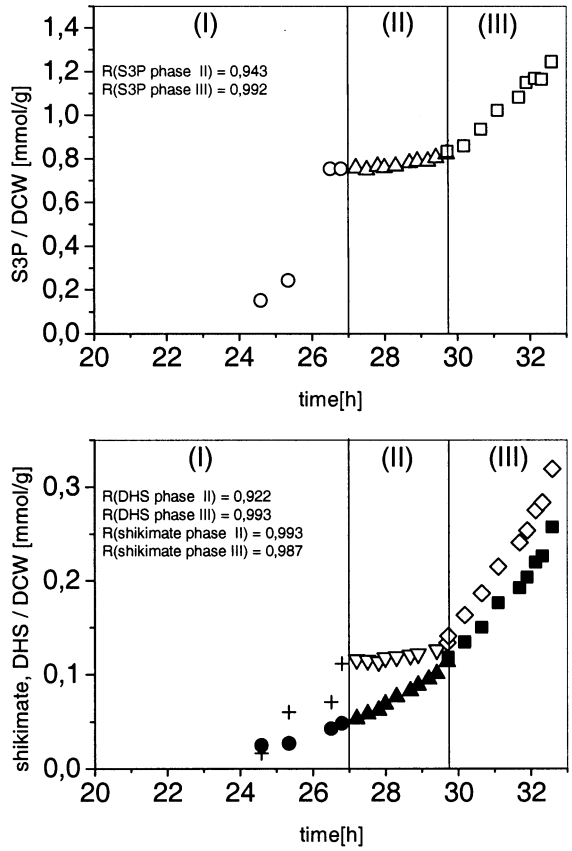

Figure 5. Biomass-specific product concentrations of *E. coli* S3P in fed-batch process with glucose pulse experiment after 75% glucose limitation; S3P in the first (○), second (△), and third (□) phase is shown, together with shikimate in the first (●), second (▲), and third (■) phase and DHS in the first (+), second (▽), and third (◇) phase, (*R*) coefficient of correlation.

product formation rates of *E. coli* DHS and *E. coli* DAH(P) at 50% glucose limitation are compared, a relatively high DHS production (approximately 74% of the maximum value) could be observed. DAH(P) production only achieved 40% of its maximum. From this we concluded that a further decrease of glucose limitation down to 25% would not show any differences in DHS formation compared to the maximum value. A 25% glucose limitation experiment for *E. coli* DHS was therefore not performed. As observed for *E. coli* DAH(P) the formation rates of *E. coli* DHS in the third phase show a high reproducibility (Table 3). In all four experiments the same final DHS formation rate of 0.647 ± 0.017 mmol DHS/(g·h) was observed.

Experiments with *E. coli* S3P. Further studies with *E. coli* S3P were carried out to investigate the glucose pulse transmission via DAH(P) and DHS downstream to S3P. Experiments with 50% and 75% limitation were performed. While the strains *E. coli* DAH(P) and *E. coli* DHS accumulate only the intermediate, which is prior to the catalytically inactive enzyme, *E. coli* S3P exhibits different behavior. Beside S3P, shikimate and DHS were also detected. Shikimate accumulation could be a consequence of an unspecific phosphatase activity taking S3P as a substrate. The appearance of DHS could be explained by a relatively low activity of shikimate dehydrogenase (AroE) that could be caused by a feedback inhibition of shikimic acid (*18*).

After the glucose pulse in the experiment with 75% limitation the production rates of S3P, shikimate and DHS increased (Figure 5, Table 4). However, it should

Table 4. Specific Production Rates for S3P, Shikimate, and DHS for *E. coli* S3P

	limitation			
	75%	0%	50%	0%
π_{DHS}[a]	0.005	0.059	0.018	0.062
$\pi_{shikimate}$[b]	0.023	0.045	0.005	0.005
π_{S3P}[c]	0.026	0.146	0.099	0.105

[a] Specific DHS production rate in mmol DHS/(g·h). [b] Specific shikimate production rate in mmol shikimate/(g·h). [c] Specific S3P production rate in mmol S3P/(g·h).

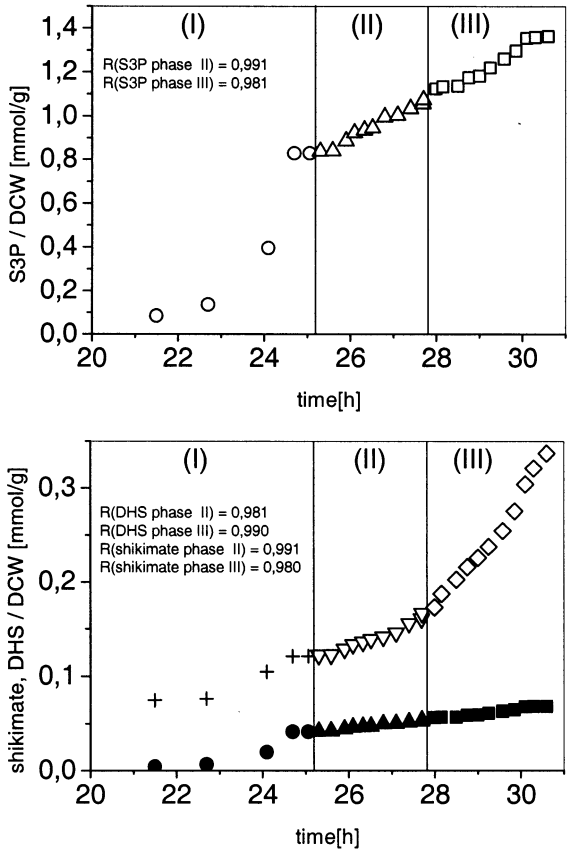

Figure 6. Biomass-specific product concentrations of *E. coli* S3P in fed-batch process with glucose pulse experiment after 50% glucose limitation; S3P in the first (○), second (△), and third (□) phase is shown, together with shikimate in the first (●), second (▲), and third (■) phase and DHS in the first (+), second (▽), and third (◇) phase; (R) coefficient of correlation.

be noticed that the significance of rate changes strongly depends on the intermediate position in the aromatic amino acid pathway. Intermediates further downstream of the pathway were less affected than those upstream. For instance, π_{DHS} increased significantly more strongly than $\pi_{shikimate}$, which could be a consequence of the feedback inhibition at increasing shikimate concentrations. Additionally, much stronger changes of π_{DHS} were observed than those of π_{S3P}. In the 75% limitation experiment the most dominant change of the production rate is observed for DHS, showing a more than 11.8-fold increase of the production rate after the pulse. In case of S3P a 5.6-fold increase could be observed while the shikimate production rate only doubled.

In the experiment with 50% limitation rate changes also depend on the intermediate position in the aromatic amino acid pathway (Figure 6, Table 4). In analogy to the 75% limitation experiment the most significant change was observed for DHS. The production rate of DHS showed a 3.4-fold increase after the glucose pulse,

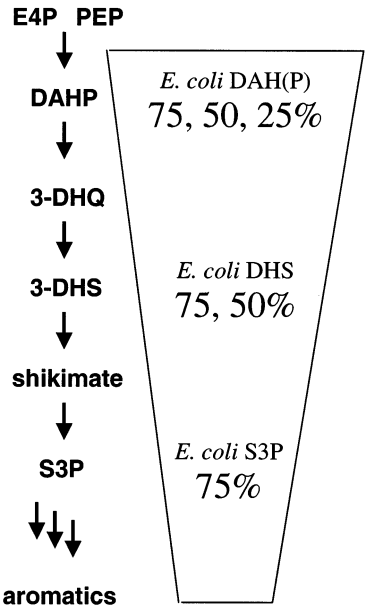

Figure 7. Pulse intensities necessary to significantly influence formation rates of DAH(P), DHS, and S3P for *E. coli* DAH(P), *E. coli* DHS, and *E. coli* S3P, respectively.

while the production rates of S3P and shikimate remain constant. In both experiments the most significant change of production rates was observed for DHS, which is the most upstream intermediate. Significantly smaller changes of the production rates were observed in both experiments for the more downstream intermediates S3P and shikimate. The observed quantitative differences between the shikimate production rates in both experiments is a surprising result, and currently studies are being carried out for further investigation on this effect.

Figure 7 gives a simplified overview of the experimental results using the different strains in glucose pulse experiments. As indicated, significant flux changes after glucose pulses could be expected in the aromatic amino acid pathway. However, their intensity strongly depended on the position of the pathway intermediate in focus. While relatively small changes of 25% glucose supply could still be detected for DAH(P), a 75% increase was necessary to influence S3P production. Besides, it should be noticed that glucose pulses did affect S3P, provided that their intensity was strong enough.

Estimation of Rapid Sampling Time Window. The above-mentioned experimental results indicated that glucose pulses are generally applicable to study metabolism dynamics in the aromatic amino acid pathway. Now, the question should be answered, whether a rapid sampling approach (sampling frequency > 1 Hz) would be necessary in order to document metabolic dynamics satisfactorily. For this reason, DO courses during glucose pulses were chosen as an indicator as a result of their known straight and fast coupling to the cells' oxygen and glucose uptake (*20*). Figure 8 shows a representative example of the whole experimental series.

Immediately after addition of glucose pulse, DO shows a steep decrease indicating an accelerated oxygen uptake rate and a higher glucose consumption rate (Figure 8). After approximately 7 min a constant DO level of about 20% was reached, indicating a new steady state for the cell metabolism. Assuming that the changes of oxygen uptake strongly correlate with metabolism dynamics (also in the aromatic amino acid pathway), high-frequency sampling on the second scale would be necessary to detect the significant changes during the first minute after

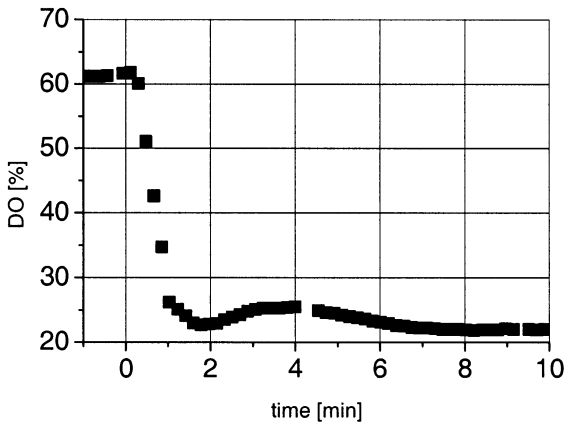

Figure 8. DO data showing increased oxygen consumption after glucose pulse addition to the 50% limited culture of *E. coli* DAH(P).

pulse. So rapid sampling technology, as presented elsewhere (*3*), is necessary to analyze further pulse experiments.

Conclusions

In this study it was shown that glucose pulse experiments can be performed reproducibly during fed-batch fermentations with different recombinant strains. The definition of limitation levels referring to a predetermined, saturated glucose consumption rate was a useful tool in order to compare different strains. The experimental technique using glucose pulses together with measurement of metabolites accumulating extracellularly worked well for the aromatic amino acid pathway. Results showed that a glucose pulse was able to shift carbon fluxes into the aromatic amino acid pathway. Because no negative, irreversible effect was observed, strong glucose limitations for about 4 h can be used before the glucose uptake shift in order to maximize the resulting metabolism response. This is necessary because glucose pulse transmission into the aromatic amino acid pathway decreased, comparing data for *E. coli* DAHP, *E. coli* DHS, and *E. coli* S3P. With respect to a potential pulse experiment with a L-phe-producing strain, this is of great importance because L-phe is synthesized even downstream of S3P, which could make a limitation stronger than 75% necessary. The successful conclusion of these preliminary experiments justifies the more intensive task of developing analytical methods, e.g., LC-MS/MS, for the determination of intracellular metabolite concentrations. The pulse technique in combination with a rapid sampling will be tested for the quantification of the aromatic amino acid pathway. With regard to in vivo measurements of metabolic dynamics, which will enable modeling of enzyme and pathway kinetics, the determination of intracellular concentrations of metabolites from the aromatic amino acid pathway is the subject of future work.

Acknowledgment

This work was funded by a BioRegio-Initiative of the German Federal Ministry of Education and Research (grant 0311644). The authors are deeply indebted to Professor Ch. Wandrey, Research Centre Jülich, Germany, for his support for this work and the excellent research conditions at the Institute of Biotechnology. The authors would like to thank PD Dr. Georg Sprenger for his advice, Mr. Marco Krämer for providing the strain

AB2829/pF84, Ms. Ursula Degner for cloning work, and Ms. Heidi Haase for HPLC measurements.

References and Notes

(1) Theobald, U.; Mailinger, W.; Baltes, M.; Rizzi, M.; Reuss, M. In Vivo Analysis of Metabolic Dynamics in *Saccharomyces cerevisiae*: I. Experimental Observations. *Biotechnol. Bioeng.* **1997**, *55*(2), 305−316.

(2) Rizzi, M.; Baltes, M.; Theobald, U.; Reuss, M. In Vivo Analysis of Metabolic Dynamics in *Saccharomyces cerevisiae*: II. Mathematical Model. *Biotechnol. Bioeng.* **1997**, *55*(4), 592−608.

(3) Schäfer, U.; Boos, W.; Takors, R.; Weuster-Botz, D. Automated Sampling Device for Monitoring Intracellular Metabolite Dynamics. *Anal. Biochem.* **1999**, *270*, 88−96.

(4) Weuster-Botz, D. Sampling Tube Device for Monitoring Intracellular Metabolite Dynamics. *Anal. Biochem.* **1997**, *246*, 1189−1195.

(5) Stephanopoulos, G.; Nielsen, J.; Aristodou, A. *Metabolic Engineering: Principles and Methodologies*; Academic Press: San Diego, 1998.

(6) de Noronha Pissara, P.; Nielsen J.; Bazin, M. J. Pathway Kinetics and Metabolic Control Analysis of a High-yielding Strain of *Penicillium chrysogenum* during Fed Batch Cultivation. *Biotechnol. Bioeng.* **1996**, *51*, 168−176.

(7) Hatzimanikatis, V.; Bailey, J. E. MCA Has More To Say. *J. Theor. Biol.* **1996**, *182*, 233−242.

(8) Budzinski, A. Aminosäuren, Peptide und die Chemie dazu. *Chem. Rundsch.* **2001**, *6*, 10.

(9) Müller, A. Hartes Gerangel um den Futtertrog. *Chem. Rundsch.* **2001**, *6*, 1.

(10) Pittard, A. J. Biosynthesis of the Aromatic Amino Acids. In *Escherichia coli and Salmonella typhimurium*; Neidhardt, F. C., Ed.; ASM Press: Washington, DC, 1996; Vol. 1, pp 458−484.

(11) Postma, P. W.; Lengeler, J. W.; Jacobson, G. R. Phosphoenolpyruvate: Carbohydrate Phosphotransferase Systems of Bacteria. *Microbiol. Rev.* **1993**, *57*(3), 543−594.

(12) Buchholz, A.; Takors, R.; Wandrey, C. Quantification of Intracellular Metabolites in *Escherichia coli* K12 using Liquid Chromatographic-Electrospray Ionization Tandem Mass Spectrometric Techniques. *Anal. Biochem.* **2001**, *295*, 129−137.

(13) Pittard, A. J.; Wallace, B. J. Distribution and Function of Genes Concerned with Aromatic Biosynthesis in *Escherichia coli*. *J. Bacteriol.* **1966**, *91*, 1494.

(14) Zeppenfeld, T.; Larisch, C.; Lengeler, J. W.; Jahreis, K. Glucose Transporter Mutants of *Escherichia coli* K-12 with Changes in Substrate Recognition of $IICB^{Glc}$ and Induction Behaviour of the *ptsG* Gene. *J. Bacteriol.* **2000**, *182*, 4443.

(15) Krämer, M. Investigations on the Influence of Increased Availability of Erythrose 4-Phosphate and Phosphoenolpyruvate on the Carbon Flux into the Aromatic Amino Acid Pathway of *Escherichia coli*. Ph.D. Thesis, University of Düsseldorf (Germany) 2000.

(16) Fürste, J. P.; Pansegrau, W.; Frank, R.; Blöcker, H.; Scholz, P.; Bagdasarian, M.; Lanka, E. Molecular Cloning of the Plasmid RP4 Primase Region in a multi-host-range tacP Expression Vector. *Gene* **1986**, *48*, 119−131.

(17) Jossek, R.; Bongaerts, J.; Sprenger, G. A. Characterization of a New Feedback-Resistant 3-Deoxy-D-*arabino*-heptulosonate 7-Phosphate Synthase AroF of *Escherichia coli*. *FEMS Microbiol. Lett.* **2001**, *202*, 145.

(18) Dell, K. A.; Frost, J. W. Identification and Removal of Impediments to Biocatalytic Synthesis of Aromatics from D-Glucose: Rate-Limiting Enzymes in the Common Pathway of Aromatic Amino Acid Biosynthesis *J. Am. Chem. Soc.* **1993**, *115*, 11581−11589.

(19) Mousdale, D. M.; Coggins, J. R. High-Performance Liquid Chromatography of Shikimate Pathway Intermediates. *J. Chromatogr.* **1985**, *329*, 268−272.

(20) Lin, H. Y.; Mathiszik, B.; Xu, B.; Enfors S.-O.; Neubauer, P. Determination of the Maximum Specific Uptake Capacities for Glucose and Oxygen in Glucose-Limited Fed-Batch Cultivations of *Escherichia coli*. *Biotechnol. Bioeng.* **2001**, *73*, 5, 347−356.

Accepted for publication July 8, 2002.

BP010199Z